DOI: 10.1002/chem.201000837

# Fluorescence Spectroscopic Evidence for Hydrogen Bonding and Deprotonation Equilibrium between Fluoride and a Thiourea Derivative

**Pichandi Ashokkumar, Vayalakkavoor T. Ramakrishnan, and Perumal Ramamurthy*[a]**

**Abstract:** Interaction of anions with thiourea-linked acridinedione fluorophore was studied by absorption, $^1$H NMR, steady-state and time-resolved fluorescence techniques. Addition of $AcO^-$ and $H_2PO_4^-$ shows a genuine H-bonded complex with thiourea receptor; whereas, $F^-$ shows stepwise H-bonding and deprotonation of thiourea NH as confirmed by $^1$H NMR titration. Free receptor **1** shows emission maximum at 418 nm; whereas, H-bonded complex of **1**·$F^-$ shows a new redshifted emission maximum at 473 nm and the deprotonated **1** exhibits an emission peak at 502 nm. Presence of these three different emitting species was probed by 3D emission spectroscopic studies. Equilibrium between the free receptor **1**, **1**·$F^-$ H-bonded complex and deprotonated **1** was confirmed by time-resolved fluorescence studies. Time-resolved area normalised emission spectra (TRANES) of **1** in the presence of $F^-$ shows two isoemissive points at 456 and 479 nm between time delays of 0–0.5 ns and 1–20 ns, respectively, due to the existence of three emitting species in equilibrium. Observation of such an equilibrium based on fluorescence spectroscopic studies further proves the earlier reported absorption and $^1$H NMR spectroscopic studies of H-bonding and deprotonation processes and also illustrates the dynamics of anion-receptor interactions.

**Keywords:** charge transfer · deprotonation · fluorescence spectroscopy · hydrogen bonds · thioureas

## Introduction

Anion recognition and sensing has recently grown into a subject of great interest in supramolecular and organic chemistry.[1] Over the past decade, various examples of hydrogen-bond donors such as urea,[2] thiourea,[3] amine,[4] amide,[5] pyrrole,[6] imidazole,[7] indole[8] moieties have been shown to be particularly effective anion receptors in organic solvents. Both hydrogen-bonding and deprotonation processes are involved in anion interaction, which depends on the basicity of the anion and acidity of the proton.[9] If the basicity of an anion $A^-$ is insufficient to induce deprotonation of the receptor RH, one observes a formation of hydrogen bonded complex R-H···$A^-$ [Eq. (1)].

$$RH + A^- \rightleftharpoons RH \cdots A^- \quad (1)$$

If the basicity is high enough, it will induce deprotonation prior to the hydrogen-bonding interaction [Eq. (2)].

$$RH + A^- \rightleftharpoons R^- + AH \quad (2)$$

In a borderline case, an anion initially forms the hydrogen-bonded complex. But with sufficiently excess of added anions, deprotonation occurs due to formation of hydrogen-bonded anion dimer $A_2H^-$ [Eq. (3)].

$$RH \cdots A^- \rightleftharpoons R^- + AHA^- \quad (3)$$

The above stepwise changes are most often observed for thiourea receptor with $F^-$ and also with $AcO^-$.[9a,c,d]

Fluorescence-based anion sensors are most attractive due to the simplicity and high detection limit of fluorescence.[10] Thus, the understanding of anion-receptor interactions from fluorescence spectroscopic studies is vital; but until now anion-receptor interactions, namely the H-bonding and deprotonation and its equilibrium, are not clearly investigated by fluorescence spectroscopic studies. Most of the reported fluorescence based sensors utilize different kind of signaling mechanism such as photoinduced electron transfer (PET),[11] intramolecular charge transfer (ICT),[12] metal-to-ligand charge transfer,[13] excimer/exciplex formation,[14] and tuning

[a] P. Ashokkumar, Prof. Dr. V. T. Ramakrishnan, Prof. Dr. P. Ramamurthy
National Centre for Ultrafast Processes, University of Madras
Taramani Campus, Chennai 600 113 (India)
Fax: (+91) 44-24546709
E-mail: prm60@hotmail.com

Supporting information for this article is available on the WWW under http://dx.doi.org/10.1002/chem.201000837.

   

of proton transfer.[15] In classical PET-based anion sensors, both H-bonding and deprotonation do not show any change in the absorption spectrum and leads to the fluorescence quenching without any spectroscopic shift. Whereas in ICT-based sensors, H-bonding interaction shows a red shift in the absorption maximum and the deprotonation leads to the formation of a new absorption band at longer wavelength. H-bonding and deprotonation processes are also observed with $^1$H NMR spectroscopic studies; H-bonding interaction shows downfield shift of the NH signals and the deprotonation leads to the disappearance of NH signals with the formation of new triplet around 16 ppm corresponding to an $FHF^-$ complex. Although the above equilibrium is observed from absorption and $^1$H NMR spectroscopic studies,[9] the detailed investigation from fluorescence spectroscopic studies has not yet been reported. Since the fluorescence-based detection will offer additional advantages such as high sensitivity of detection down to the single molecule, local observation by fluorescence imaging with subnanometer spatial resolution and remote sensing by using optical fibers with a molecular sensor immobilized at the tip,[16] the detailed investigation from fluorescence spectroscopy will further expand the fluorescence based anion detection. Herein, we have carried out steady-state and time-resolved fluorescence studies to probe the H-bonding and deprotonation equilibrium of anions with thiourea linked acridinedione (ADD) derivative **1** (ADDTU). Since both PET and ICT mechanisms can operate in ADD, it will be good to use it as a signaling unit in sensor molecules.[17] In the present sensor molecule **1**, the thiourea receptor is linked through conjugation with the ADD chromophore. Thus, any variation in the electron density of the thiourea receptor will alter the ICT of the chromophore and results in a shift in both absorption and emission maxima. Interestingly, three different emission maxima are observed with the addition of $F^-$, which correspond to free ADDTU **1**, H-bonded complex of **1**·$F^-$ and deprotonated species of **1**. In addition to the previous absorption and $^1$H NMR spectroscopic studies on the discrimination of the H-bonding and deprotonation processes, the present fluorescence studies clearly illustrates the dynamics of anion-receptor interactions.

## Results and Discussion

**Synthesis**: The thiourea-linked ADD derivative (**1**) was synthesized by refluxing tetraketone **1a** with thiosemicarbazide in acetic acid as shown in Scheme 1.

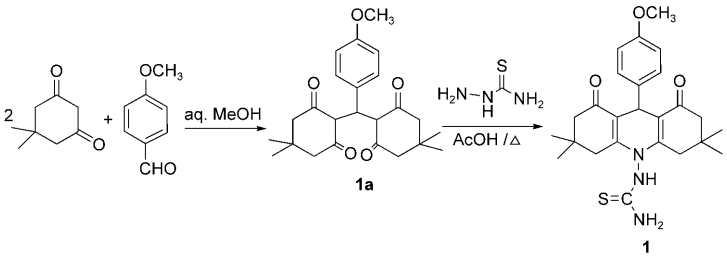


Scheme 1. Synthesis of ADDTU (**1**).

**Photophysical studies of 1**: Compound **1** shows the absorption and emission maxima at 363 and 418 nm, respectively, in acetonitrile, which are assigned to the ICT from the ring nitrogen atom to the ring carbonyl center within the ADD moiety. Fluorescence quantum yield and lifetime were found to be 0.03 (±2%) and 0.35 ns (±0.02), respectively, in acetonitirile. Lower fluorescence quantum yield and lifetime of **1** compared with the constituent fluorophore without electron donor $OCH_3$ moiety at the nineth position ($\phi_f = 0.63 \pm 2\%$ and $\tau_f = 5.2 \pm 0.01$ ns) are attributed to the intramolecular PET process through space from the electron rich $OCH_3$ group to the relatively electron deficient excited state of the ADD fluorophore.[18]

**$AcO^-$ and $H_2PO_4^-$ binding studies**: Addition of $AcO^-$ to the acetonitrile solution of **1** shows a 6 nm redshifted absorption maximum with an isosbestic point at 366 nm as shown in Figure 1a. The observed red shift in the absorption maximum indicates the H-bonding interaction of $AcO^-$ with 1:1 complexation, which is evident from the observed isosbestic point. The corresponding fluorescence spectrum, when excited at its isosbestic point, shows the formation of a new redshifted emission peak at 484 nm with fluorescence enhancement (Figure 1b). The binding constant was estimated to be 3275 $M^{-1}$ from the linear relationship obtained in the Benesi–Hildebrand plot[19] (Figure 2).

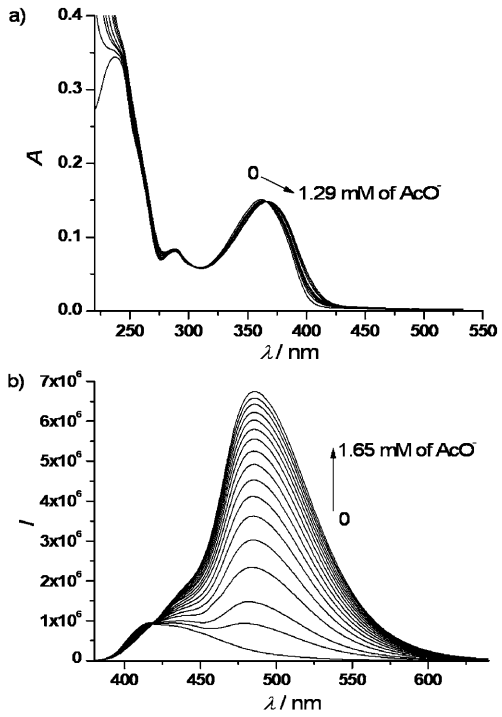


Figure 1. a) Absorption and b) emission spectroscopic changes of **1** (12 μM) upon addition of $AcO^-$ in acetonitrile; $\lambda_{ex} = 366$ nm.

  

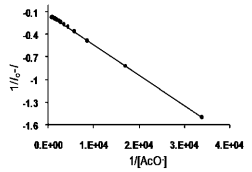


Figure 2. Benesi–Hildebrand plot for **1** (12 μM) upon addition of $AcO^-$ in acetonitrile; $\lambda_{ex}=366$ nm; $\lambda_{em}$ monitored at 484 nm.

Addition of $H_2PO_4^-$ also shows a similar behavior with a 5 nm redshifted absorption maximum and a new redshifted emission peak at 436 nm with fluorescence enhancement (Figure S3). $H_2PO_4^-$ shows (Figure S4) a lower binding constant ($1678\ M^{-1}$) than $AcO^-$. Addition of $AcO^-$ and $H_2PO_4^-$ results in the hydrogen-bonding interaction with the thiourea NH, thereby increasing the electron density of the donor group of the ICT chromophore. This increase in the charge density leads to the redshift of absorption and the formation of the new redshifted emission peak together with an increase in the intensity. The extent of redshift depends on the charge density of anions, which accounts for the observed redshift for $AcO^-$ and $H_2PO_4^-$.

**$F^-$-binding studies**: In contrast to the results obtained with $AcO^-$ and $H_2PO_4^-$, addition of $F^-$ shows two stepwise changes in the absorption spectrum of **1** as shown in Figure 3a. At lower concentration of $F^-$ (up to 0.1 mM), a 12 nm red shifted absorption maximum with isosbestic points at 315 and 385 nm is observed; whereas at higher concentration, a new absorption peak at 459 nm is formed with isosbestic points at 315 and 401 nm. Similar to $AcO^-$ and $H_2PO_4^-$, H-bonded complex of $F^-$ shows the red shift in the absorption maximum, but the deprotonation of the thiourea NH leads to the formation of a new peak, which is confirmed by observing similar peak on the addition of $HO^-$ (Figure S5a).

After observing a different response of H-bonded and deprotonated species from absorption spectroscopic studies, we carried out fluorescence spectroscopic studies (Figure 3b) by excitation at its isosbestic point. Addition of $F^-$ results in the formation of a new peak at 473 nm followed by a peak at 502 nm. At higher concentration of $F^-$, the intensity of 502 nm peak increases at the expense of 473 nm peak. H-bonded complex of **1**·$F^-$ shows a peak at 473 nm; whereas, the deprotonation leads to the formation of another new emission peak at 502 nm. To confirm this observation, we carried out similar experiment with the addition of $HO^-$, which also shows a new emission peak at 502 nm at the expense of 418 nm peak (Figure S5b). $HO^-$ is a well known deprotonating agent, which can deprotonate the thiourea NH without a hydrogen-bonding complex as shown in Equation (2). Absence of 473 nm peak with the addition of $HO^-$ confirms that this peak is originated from the **1**·$F^-$ H-bonded complex. To probe the origin of the excitation of these emitting species, we have carried out excitation spectroscopic studies of **1** in the presence of $F^-$. Figure 4 presents the excitation spectra of **1** in the presence of 0.30 mM of $F^-$. Three different excitation maximum at 364, 387 and 458 nm are observed when they were monitored at emission maximum of 418, 473 and 502 nm, respectively. The 364 nm excitation maximum matches with the absorption maximum of free ADDTU **1**; excitation maximum at 458 nm is similar with the absorption maximum of deprotonated **1**. Whereas, the **1**·$F^-$ H-bonded complex shows redshifted excitation maximum compared to its absorption maximum. Since the absorption of both the H-bonded and deprotonated species are overlapping in that region, a clear absorption maximum could not be observed. Existence of above three emitting species and their excitation wavelength are further confirmed by 3D emission spectroscopic studies as shown in Figure 5.

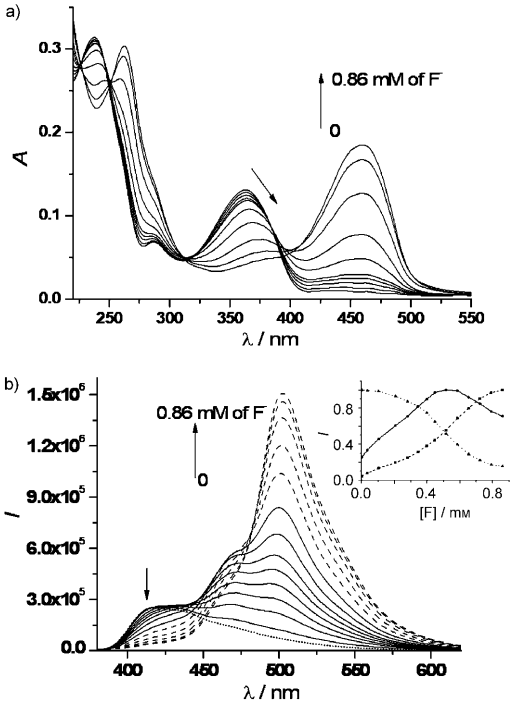


Figure 3. a) Absorption, b) emission spectroscopic changes of **1** (12 μM) upon addition of $F^-$ in acetonitrile; $\lambda_{ex}=315$ nm; inset of b) normalised emission intensity at three different wavelengths versus concentration of $F^-$: λ: ■ 502, ● 472, ▲ 418 nm.

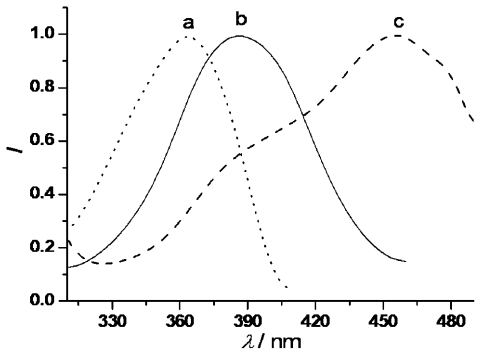


Figure 4. Excitation spectra of **1** (12 μM) with $F^-$ (0.30 mM) in acetonitrile; $\lambda_{em}$ at a) 418 nm, b) 473 nm, c) 502 nm.

  

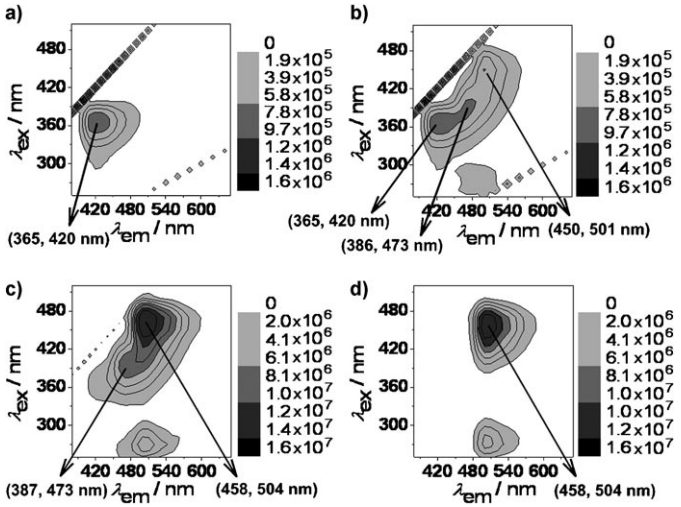


Figure 5. 3D emission spectroscopic contour plot of a) **1** alone (12 μM), b) **1** + $F^-$ (0.10 mM), c) **1** + $F^-$ (0.40 mM) & d) **1** + $F^-$ (0.80 mM) in acetonitrile.

Compound **1** shows a contour at an excitation wavelength of 365 nm and emission wavelength of 420 nm. Addition of 0.10 mM of $F^-$ shows three contours centered at excitation, emission wavelength of 365, 420 nm; 386, 473 nm and 450, 501 nm. The presence of above three contours confirms the existence three different emitting species namely free ADDTU **1**, H-bonded complex of **1**·$F^-$ and deprotonated **1**, respectively. Further increase in the concentration of $F^-$ (0.40 mM), shows the disappearance of contour of free **1** with increase in the intensity of the other two contours. At higher concentration of $F^-$ (0.80 mM), only one contour of deprotonated **1** is observed with higher intensity. This clearly shows that at lower concentration of $F^-$, H-bonded complex is formed from the free receptor **1**; and at higher concentration, deprotonated species is formed from the H-bonded complex of **1**·$F^-$. Addition of other anions like $Cl^-$, $Br^-$, $I^-$, $HSO_4^-$, $ClO_4^-$ did not show any such changes in both absorption and emission spectra.

**Time-resolved fluorescence studies**: Time-resolved emission spectroscopy (TRES) provides information on the excited state kinetics and heterogeneity of different emissive species in a system.[20] The H-bonding complexation and deprotonation have been investigated by time resolved fluorescence studies to understand the excited state behavior of these species. Figure 6a and b present the fluorescence decay of **1** with different concentrations of $F^-$ monitored at 473 and 502 nm, respectively. When the decay was monitored at 473 nm, compound **1** shows a biexponential behaviour with lifetime of 0.35 ns (88.5%) and 2.81 ns (11.5%). During the addition of $F^-$, both the components disappear gradually, with the formation of a new longer lifetime component (6.93 ns) along with an increase in the amplitude. When the concentration of $F^-$ reaches 0.22 mM, the decay was found to be single exponential with longer lifetime component (6.93 ns), and at the higher concentration of $F^-$ the lifetime remains unchanged. When the decay was monitored at 502 nm, compound **1** shows similar biexponential behaviour with the lifetime of 0.35 ns (84.7%) and 2.81 ns (15.3%). Up to 0.22 mM of $F^-$, the fluorescence decay profile of **1** show a similar behavior as observed at the wavelength of 473 nm; whereas at higher concentrations, the new longer lifetime is further increased to 8.12 ns (Figure 6b, inset). Addition of $HO^-$ also shows a longer lifetime of 8.12 ns (Figure S8), which confirms that this lifetime, is corresponding to the deprotonated **1**.

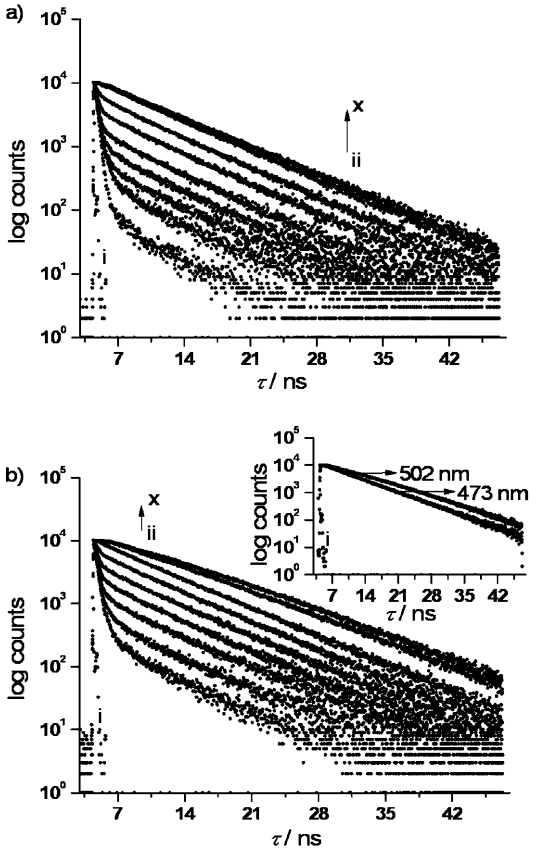


Figure 6. Fluorescence decay profiles of **1** (12 μM) with the addition of $F^-$ in acetonitrile; $\lambda_{ex}$ = 393 nm; a) $\lambda_{em}$ at 473 nm; i) lamp profile, ii) 0, iii) 0.013, iv) 0.020, v) 0.030, vi) 0.043, vii) 0.097, viii) 0.151, ix) 0.224 and x) 0.820 mM of $F^-$; b) $\lambda_{em}$ at 502 nm; i) lamp profile, ii) 0, iii) 0.020, iv) 0.030, v) 0.043, vi) 0.097, vii) 0.151, viii) 0.224, ix) 0.452 and x) 0.820 mM of $F^-$. Inset of b): Decay of **1** with 0.820 mM of $F^-$ when monitored at different emission wavelengths.

To get further insight into the presence of three emission species, we have constructed TRES and TRANES as reported earlier.[20a] Figure 7 shows the emission spectra of **1** in the presence of 0.20 mM of $F^-$ at different time delays. Immediately after the excitation (0 ns delay), TRES shows a maximum at 473 nm, which correspond to **1**·$F^-$ H-bonded complex. In addition to this, higher intensity is also seen in the region 400–440 nm, which is due to the free receptor **1**. The above observations indicate the presence of free **1** and **1**·$F^-$ H-bonded complex. After 0.75 ns delay, the intensity around

  

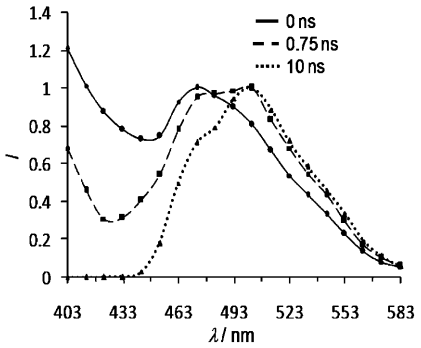


Figure 7. Emission spectra of **1** (12 μM) in the presence of 0.20 mM of $F^-$ at different time delays in acetonitrile; $\lambda_{ex}=393$ nm.

400–440 nm decreases and a new peak is observed at 502 nm (in addition to the peak at 473 nm), which is due to the deprotonated **1**. Whereas after 10 ns delay, intensity at 400–440 nm is reduced almost to zero; and the intensity of 473 nm peak is also lower than 502 nm peak. The difference in the lifetime of the above three species, leads to the time dependent peak maximum in the TRES studies. This clearly shows the presence of free **1**, **1**·$F^-$ H-bonded complex and deprotonated **1**. TRANES of **1** in the presence of $F^-$ also supports the existence of three emission species. Figure 8a and 8b show the TRANES between the time intervals of 0–0.5 and 1–20 ns, respectively. Figure 8a shows an isoemissive point at 456 nm, which is due to the existence of free ADDTU **1** and **1**·$F^-$ H-bonded complex. Figure 8b shows another isoemissive point at 479 nm, which is due to the existence of **1**·$F^-$ H-bonded complex and deprotonated **1**. Thus the heterogeneity in the excited state is clearly proved from TRES and TRANES studies, which is in good agreement with the results obtained in the steady state fluorescence studies.

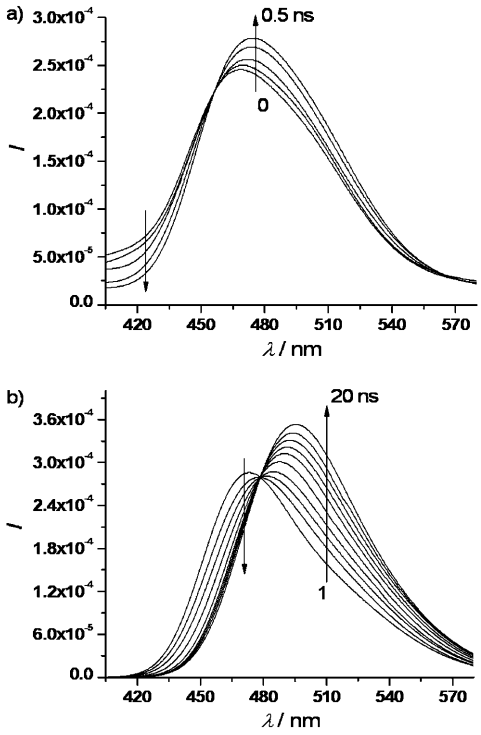


Figure 8. TRANES of **1** (12 μM) in the presence of 0.30 mM of $F^-$ a) between 0-0.5 ns, b) 1-20 ns time delay in acetonitrile; $\lambda_{ex}=393$ nm.

Addition of $AcO^-$ also shows the similar kind of lifetime decay profile as observed in **1**·$F^-$ (monitored at 473 nm). On complete complexation of **1** with $AcO^-$ shows a single exponential decay with the lifetime of 5.68 ns (Figure S9). Whereas in the presence of $H_2PO_4^-$, such a complete complexation is not observed. Even after the addition of higher concentrations of $H_2PO_4^-$, the fluorescence decay was found to be triexponential with the lifetime of 0.35 ns (6.0%), 2.81 ns (7.8%) and 4.67 ns (86.2%) (Figure S10). This clearly indicates that the H-bonding interaction of $H_2PO_4^-$ with the thiourea receptor is relatively weak, when compared to $F^-$ and $AcO^-$. Therefore the free ADDTU **1** exists in the system in addition to the H-bonded complex of **1**.$H_2PO_4^-$.

**$^1$H NMR titration with $F^-$**: Further insights into the two-step process and nature of receptor–anion interactions were provided by $^1$H NMR titration studies. Figure 9 displays the

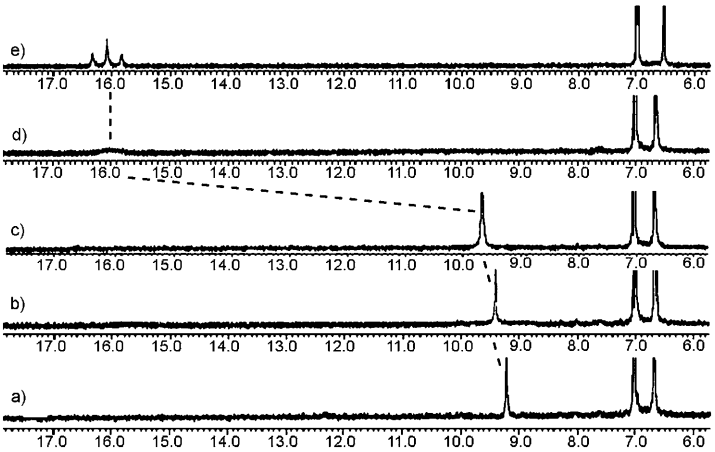


Figure 9. Stack plot of $^1$H NMR spectra of **1** (8.0 mM) with a) 0, b) 0.5, c) 1.0, d) 1.5 and e) 2.0 equivalents of $F^-$ in [$D_6$]DMSO.

NMR titration spectra of **1** with $F^-$ at 24 °C. Addition of one equivalent of $F^-$ results in the broadening and downfield shift ($\Delta\delta=0.52$ ppm) of the thiourea NH proton from $\delta$ 9.21 ppm due to the H-bonding complexation with the thiourea receptor. Addition of second equivalent of $F^-$ shows disappearance of the NH signal with the formation of a characteristic triplet around 16.1 ppm due to the formation of $FHF^-$.[21]

Addition of one equivalent of $AcO^-$ (Figure 10) also shows similar downfield shift ($\Delta\delta=0.48$ ppm) of thiourea NH proton; whereas, the addition of excess amount of $AcO^-$ did not show any further change in the spectrum. This clearly proves that the addition of $F^-$ causes initial H-bonding followed by the deprotonation of thiourea NH.

  

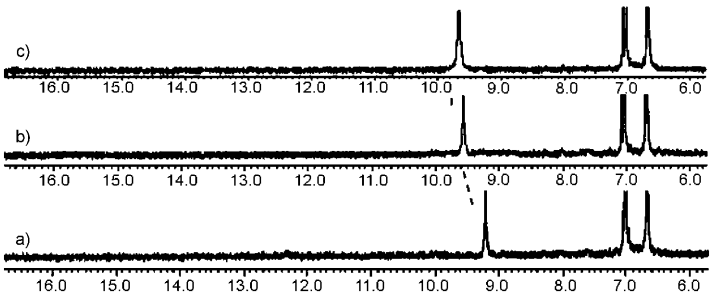


Figure 10. Stack plot of $^1$H NMR spectra of **1** (8.0 mM) with a) 0, b) 1 and c) 2.0 equivalents of $AcO^-$ in [$D_6$]DMSO.

While $AcO^-$ results in the pure H-bonding without any deprotonation due to its lower basicity compared to $F^-$.

**Binding mode of anions**: From all of the above studies, it is clear that addition of $AcO^-$ and $H_2PO_4^-$ shows H-bonding interaction with thiourea receptor; whereas, addition of $F^-$ shows stepwise H-bonding and deprotonation as shown in Scheme 2. Substitution of H instead of thiourea group in the

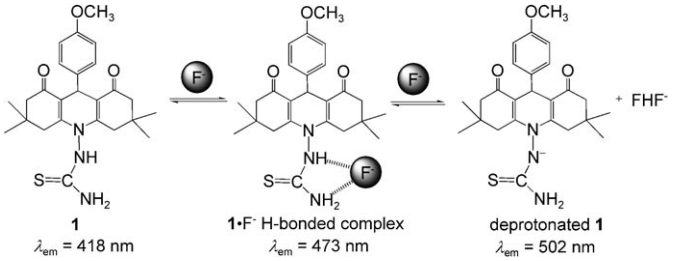


Scheme 2. Binding mode of $F^-$ with ADDTU (**1**).

ring nitrogen shows the deprotonation of ring amino hydrogen without any H-bonding complex [Eq. (2)] in the presence of $F^-$, which clearly reveals the importance of thiourea receptor in the formation of stable H-bonding complex at the lower concentration of $F^-$. The formation of **1**·$F^-$ H-bonded complex is observed even in highly polar solvent like DMSO, which also shows similar trend as observed in acetonitrile. ADDTU **1**, H-bonded complex **1**·$F^-$ and deprotonated **1** will have different charge density on N atom (ICT donor), which causes red shift in the emission maximum to different extent.

## Conclusion

A detailed steady-state and time-resolved fluorescence studies of anion–receptor interactions were carried out to understand the fluorescence response of different species present in the system. H-bonding complex of $AcO^-$ and $H_2PO_4^-$ show a new emission peak at the red shifted region depending on their basicity. Whereas $F^-$ shows two new emission peaks due to the stepwise H-bonding and deprotonation. Presence of three different emission species was probed by 3D emission spectra, TRES and TRANES studies. The observed spectroscopic changes and its interpretation were further confirmed by $^1$H NMR titration. The present investigation from fluorescence studies clearly supports the earlier report of absorption and $^1$H NMR studies for the differentiation of H-bonding and deprotonation processes. Further, it explains the equilibrium of these species hitherto unravelled in the fluorescent anion sensor. If the binding is high enough, fluorescent sensor can detect guest species down to the femtomolar concentration range. Thus future anion recognition chemistry should use more fluorescence-based detection compared with other techniques.

## Experimental Section

**General procedures and materials**: Dimedone was purchased from Alfa Aesar Pvt. Ltd.; thiosemicarbazide and all anions, as their tetrabutylammonium salts, were purchased from Sigma Aldrich Chemicals Pvt. Ltd., and were used as received. All the solvents used in the present study were of HPLC grade and purchased from Qualigens India Ltd. Absorption spectra were recorded on Agilent 8453 diode array spectrophotometer. Emission, excitation and 3D emission spectra were recorded on HORIBA JOBIN YVON Fluoromax 4P spectrophotometer. Fluorescence quantum yield was determined by exciting the sample at 366 nm with the use of quinine sulphate as the standard ($\phi_f = 0.546$ in 0.1 N $H_2SO_4$). Fluorescence decays were recorded by using an IBH time-correlated single-photon counting technique as reported elsewhere.[17b] NMR spectra were recorded on Bruker Avance III 500 MHz and JEOL 500 MHz instruments in deuterated solvents as indicated; the residual solvent peaks were used as internal standards. Chemical shifts are reported in ppm and coupling constants ($J_{X\text{-}X'}$) are reported in Hz. ESI-MS were performed on an ECA LCQ Thermo system with ion-trap detection in positive and negative mode. Elemental analyses (C, H and N) were taken on a Euro EA Elemental analyzer.

**4-Methoxybenzylidene bisdimedone (1a)**: To a solution of dimedone (4 g, 28.5 mmol) in aq. methanol (20 mL) was added 4-methoxybenzaldehyde (1.75 mL, 14.4 mmol) and warmed until the solution became cloudy. Bisdimedone **1a** started to separate. The reaction mixture was diluted with water (100 mL) and allowed to stand overnight; the tetraketone **1a** was collected by filtration, dried and recrystallized from methanol to yield pure **1a** (5.36 g, 94%). M.p. 186–187 °C.

***N*-[9-(4-Methoxyphenyl)-3,3,6,6-tetramethyl-3,4,6,7,9,10-hexahydro-1,8-(2*H*,5*H*)acridinedione-10-yl]thiourea (1)**: A mixture of the tetraketone **1a** (1 g, 2.5 mmol) and thiosemicarbazide (0.23 g, 2.5 mmol) was kept reflux in acetic acid (15 mL) for 14 h. The reaction mixture was cooled and poured into crushed ice. The solid obtained was purified by column chromatography over silica gel and eluted with $CHCl_3$: MeOH (96:4, v/v) to isolate the pure ADDTU **1** (0.83 g, 73%) as a brown powder. M.p. 208–210 °C; $^1$H NMR (500 MHz, [$D_6$]DMSO, 24 °C): $\delta = 9.26$ (s, 1H, exchanged with $D_2O$; NH), 7.05 (d, $J = 8.5$ Hz, 2H; ArH), 6.71 (d, $J = 8.5$ Hz, 2H; ArH), 4.74 (s, 1H; CH(9)), 3.91 (s, 2H, exchanged with $D_2O$; $NH_2$), 3.66 (s, 3H; $CH_3$), 2.29–2.45 (2d, $J = 17$ Hz, 4H; $CH_2$(2&7)), 1.96–2.18 (2d, $J = 16$ Hz, 4H; $CH_2$(4&5)), 0.86, 1.00 ppm (2s, 12H; $2CH_3$); $^{13}$C NMR (125 MHz, [$D_6$]DMSO, 24 °C): $\delta = 194.9$ (CO), 181.1 (CS), 157.5 (C(Ar)), 149.5 (C=C), 140.0 (C(Ar)), 129.0 (CH(Ar)), 113.4 (CH(Ar)), 112.2 (C=C), 55.3 ($CH_3$), 50.7 ($CH_2$(2&7)), 40.4 ($CH_2$(4&5)), 32.6 (CH(9)), 32.3 (C), 29.6 & 26.9 ($CH_3$); IR (KBr): $\tilde{\nu} = 3467$ ($-NH_2$), 1626 (conj. C=O), 1367 (conj. C=C) $cm^{-1}$; ESI-MS: $m/z$: 454.3 $[M+H]^+$; elemental analysis calcd (%) for $C_{25}H_{31}N_3O_3S_1$: C 66.20, H 8.48, N 6.89; found: C 66.31, H 8.46, N 6.85.

  

## Acknowledgements

We thank the Department of Science and Technology (DST), Government of India, for financial support through SERC Scheme project no. DST/SR/S1/PC-31/2005. Financial support by DST-IRHPA is also gratefully acknowledged.

[1] a) P. D. Beer, P. A. Gale, *Angew. Chem.* **2001**, *113*, 502–532; *Angew. Chem. Int. Ed.* **2001**, *40*, 486–516; b) V. Amendola, M. Bonizzoni, D. Esteban-Gomez, L. Fabbrizzi, M. Licchelli, F. Sancenon, A. Taglietti, *Coord. Chem. Rev.* **2006**, *250*, 1451–1470; c) J. L. Sessler, P. A. Gale, W. S. Cho, *Anion Receptor Chemistry*, RSC, Cambridge, **2006**; d) M. Cametti, K. Rissanen, *Chem. Commun.* **2009**, 2809–2829; e) C. Caltagirone, P. A. Gale, *Chem. Soc. Rev.* **2009**, *38*, 520–563.

[2] a) D. E. Gómez, L. Fabbrizzi, M. Licchelli, E. Monzani, *Org. Biomol. Chem.* **2005**, *3*, 1495–1500; b) E. J. Cho, B. J. Ryu, Y. J. Lee, K. C. Nam, *Org. Lett.* **2005**, *7*, 2607–2609; c) Y. J. Kim, H. Kwak, S. J. Lee, J. S. Lee, H. J. Kwon, S. H. Nam, K. Lee, C. Kim, *Tetrahedron* **2006**, *62*, 9635–9640.

[3] a) D. A. Jose, D. K. Kumar, B. Ganguly, A. Das, *Org. Lett.* **2004**, *6*, 3445–3448; b) T. Gunnlaugsson, P. E. Kruger, P. Jensen, J. Tierney, H. D. P. Ali, G. M. Hussey, *J. Org. Chem.* **2005**, *70*, 10875–10878; c) V. Thiagarajan, P. Ramamurthy, *Spectrochim. Acta Part A* **2007**, *67*, 772–777; d) W. X. Liu, Y. B. Jiang, *J. Org. Chem.* **2008**, *73*, 1124–1127; e) R. M. Duke, J. E. O'Brien, T. McCabe, T. Gunnlaugsson, *Org. Biomol. Chem.* **2008**, *6*, 4089–4092.

[4] V. Thiagarajan, P. Ramamurthy, *J. Lumin.* **2007**, *126*, 886–892.

[5] a) C. R. Bondy, S. J. Loeb, *Coord. Chem. Rev.* **2003**, *240*, 77–99; b) M. J. Chmielewski, J. Jurczak, *Chem. Eur. J.* **2005**, *11*, 6080–6094; c) S. O. Kang, R. A. Begum, K. Bowman-James, *Angew. Chem.* **2006**, *118*, 8048–8061; *Angew. Chem. Int. Ed.* **2006**, *45*, 7882–7894.

[6] a) P. A. Gale, *Chem. Commun.* **2005**, 3761–3772; b) J. L. Sessler, D. E. Gross, W. S. Cho, V. M. Lynch, F. P. Schmidtchen, G. W. Bates, M. E. Light, P. A. Gale, *J. Am. Chem. Soc.* **2006**, *128*, 12281–12288; c) C. I. Lin, S. Selvi, J. M. Fang, P. T. Chou, C. H. Lai, Y. M. Cheng, *J. Org. Chem.* **2007**, *72*, 3537–3542; d) C. H. Lee, H. Miyaji, D. W. Yoon, J. L. Sessler, *Chem. Commun.* **2008**, 24–34.

[7] a) X. Peng, Y. Wu, J. Fan, M. Tian, K, Han, *J. Org. Chem.* **2005**, *70*, 10524–10531; b) K. Chellappan, N. J. Singh, I. C. Hwang, J. W. Lee, K. S. Kim, *Angew. Chem.* **2005**, *117*, 2959–2963; *Angew. Chem. Int. Ed.* **2005**, *44*, 2899–2903.

[8] a) F. M. Pfeffer, K. F. Lim, K. J. Sedgwick, *Org. Biomol. Chem.* **2007**, *5*, 1795–1799; b) P. A. Gale, *Chem. Commun.* **2008**, 4525–4540.

[9] a) M. Boiocchi, L. Del Boca, D. Esteban- Gomez, L. Fabbrizzi, M. Licchelli, E. Monzani, *J. Am. Chem. Soc.* **2004**, *126*, 16507–16514; b) M. Boiocchi, L. Del Boca, D. Esteban-Gomez, L. Fabbrizzi, M. Licchelli, E. Monzani, *Chem. Eur. J.* **2005**, *11*, 3097–3104; c) D. Esteban-Gómez, L. Fabbrizzi, M. Licchelli, E. Monzani, *Org. Biomol. Chem.* **2005**, *3*, 1495–1500; d) V. Amendola, D. Esteban-Gomez, L. Fabbrizzi, M. Licchelli, *Acc. Chem. Res.* **2006**, *39*, 343–353; e) M. Bonizzoni, L. Fabbrizzi, A. Taglietti, F. Tiengo, *Eur. J. Org. Chem.* **2006**, 3567–3574; f) J. V. Ros-Lis, R. Martinez-Manez, F. Sancenon, J. Soto, K. Rurack, H. Weibhoff, *Eur. J. Org. Chem.* **2007**, 2449–2458; g) F. Han, Y. Bao, Z. Yang, T. M. Fyles, J. Zhao, X. Peng, J. Fan, Y. Wu, S. Sun, *Chem. Eur. J.* **2007**, *13*, 2880–2892; h) C. Pérez-Casas, A. K. Yatsimirsky, *J. Org. Chem.* **2008**, *73*, 2275–2284.

[10] A. P. de Silva, H. Q. N. Gunaratne, T. Gunnlaugsson, A. J. M. Huxley, C. P. McCoy, J. T. Rademacher, T. E. Rice, *Chem. Rev.* **1997**, *97*, 1515–1566.

[11] a) S. K. Kim, J. Yoon, *Chem. Commun.* **2002**, 770–771; b) T. Gunnlaugsson, A. P. Davis, J. E. O'Brien, M. Glynn, *Org. Lett.* **2002**, *4*, 2449–2452; c) T. Gunnlaugsson, H. D. P. Ali, M. Glynn, P. E. Kruger, G. M. Hussey, F. M. Pfeffer, C. M. G. dos Santos, J. Tierney, *J. Fluoresc.* **2005**, *15*, 287–299; d) W. X. Liu, Y. B. Xiang, *Org. Biomol. Chem.* **2007**, *5*, 1771–1775; e) E. B. Veale, T. Gunnlaugsson, *J. Org. Chem.* **2008**, *73*, 8073–8076.

[12] a) A. Kovalchuk, J. L. Bricks, G. Reck, K. Rurack, B. Schulz, A. Szumna, H. Weibhoff, *Chem. Commun.* **2004**, 1946–1947; b) F. Y. Wu, Z. Li, L. Guo, X. Wang, M. H. Lin, Y. F. Zhao, Y. B. Jiang, *Org. Biomol. Chem.* **2006**, *4*, 624–630; c) E. Quinlan, S. E. Matthews, T. Gunnlaugsson, *J. Org. Chem.* **2007**, *72*, 7497–7503; d) J. Shao, H. Lin, H. Lin, *Talanta* **2008**, *77*, 273–277.

[13] a) V. Amendola, E. Bastianello, L. Fabbrizzi, C. Mangano, P. Pallavicini, A. Perotti, A. M. Lanfredi, F. Ugozzoli, *Angew. Chem.* **2000**, *112*, 3039–3042; *Angew. Chem. Int. Ed.* **2000**, *39*, 2917–2920; b) P. Anzenbacher, Jr., D. S. Tyson, K. Jursikova, F. N. Castellano, *J. Am. Chem. Soc.* **2002**, *124*, 6232–6233.

[14] a) S. K. Kim, J. H. Bok, R. A. Bartsch, J. Y. Lee, J. S. Kim, *Org. Lett.* **2005**, *7*, 4839–4842; b) H. K. Cho, D. H. Lee, J. I. Hong, *Chem. Commun.* **2005**, 1690–1692; c) A. Pramanik, G. Das, *Tetrahedron* **2009**, *65*, 2196–2200.

[15] a) X. He, S. Hu, K. Liu, Y. Guo, J. Xu, S. Shao, *Org. Lett.* **2006**, *8*, 333–336; b) Y. Wu, X. Peng, J. Fan, S. Gao, M. Tian, J. Zhao, S. Sun, *J. Org. Chem.* **2007**, *72*, 62–70; c) X. F. Yang, H. Qi, L. Wang, Z. Su, G. Wang, *Talanta* **2009**, *80*, 92–97; d) H. S. Jung, H. J. Kim, J. Vicens, J. S. Kim, *Tetrahedron Lett.* **2009**, *50*, 983–987.

[16] *Chemosensors for Ion and Molecule Recognition* (Eds.: J. P. Desvergne, A. W. Czarnik), Kluwer Academic, Dordrecht, **1997**.

[17] a) V. Thiagarajan, P. Ramamurthy, D. Thirumalai, V. T. Ramakrishnan, *Org. Lett.* **2005**, *7*, 657–660; b) P. Ashokkumar, V. T. Ramakrishnan, P. Ramamurthy, *Eur. J. Org. Chem.* **2009**, 5941–5947.

[18] a) V. Thiagarajan, C. Selvaraju, E. J. Padma Malar, P. Ramamurthy, *ChemPhysChem* **2004**, *5*, 1200–1209; b) R. Kumaran, P. Ramamurthy, *J. Phys. Chem. B* **2006**, *110*, 23783–23789; c) V. Thiagarajan, V. K. Indirapriyadharshini, P. Ramamurthy, *J. Inclusion Phenom. Macrocyclic Chem.* **2006**, *56*, 309–313; d) P. Ashokkumar, V. Thiagarajan, S. Vasanthi, P. Ramamurthy, *J. Photochem. Photobiol. A* **2009**, *208*, 117–124.

[19] a) H. A. Benesi, J. H. Hildebrand, *J. Am. Chem. Soc.* **1949**, *71*, 2703–2707; b) V. K. Indirapriyadharshini, P. Karunanithi, P. Ramamurthy, *Langmuir* **2001**, *17*, 4056–4060.

[20] a) A. S. R. Koti, M. M. G. Krishna, N. Periasamy, *J. Phys. Chem. A* **2001**, *105*, 1767–1771; b) A. S. R. Koti, N. Periasamy, *J. Chem. Phys.* **2001**, *115*, 7094–7099.

[21] I. G. Shenderovich, H. H. Limbach, S. N. Smirnov, P. M. Tolstoy, G. S. Denisov, N. S. Golubev, *Phys. Chem. Chem. Phys.* **2002**, *4*, 5488–5497.

Received: April 2, 2010
Published online: October 4, 2010

  